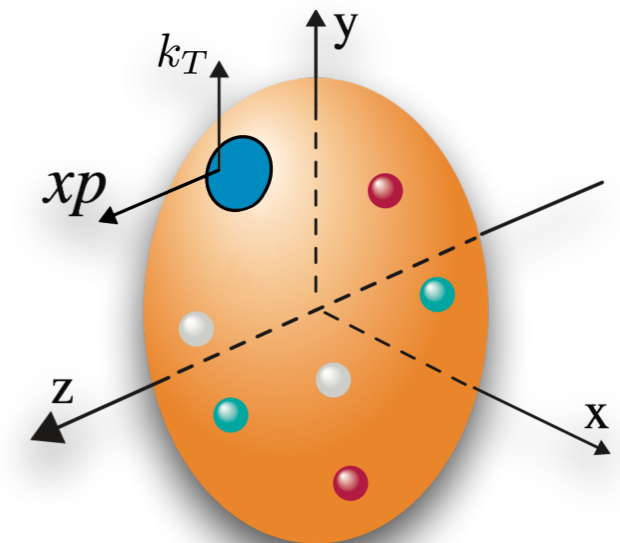
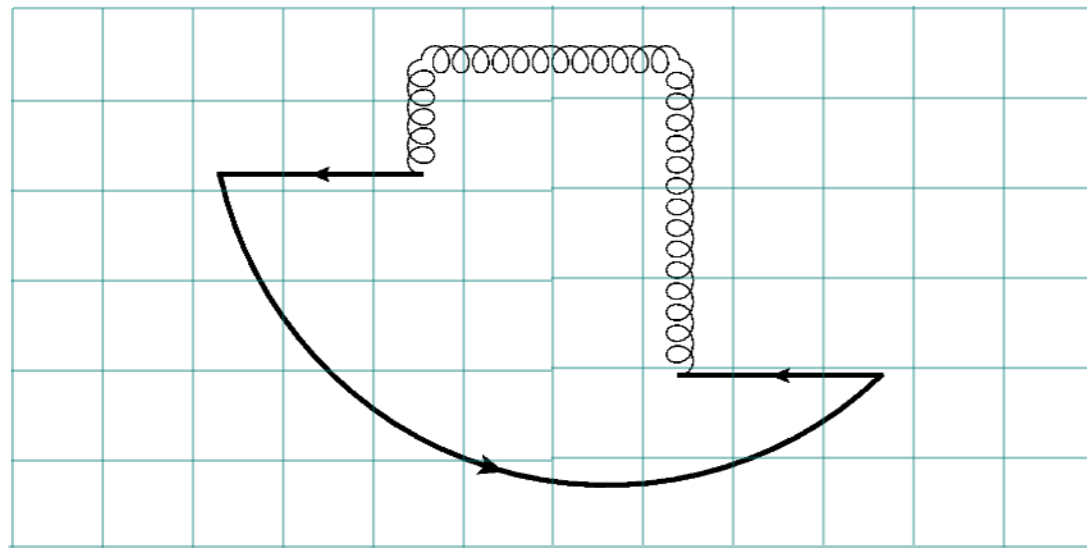


# Computing the Collins-Soper Kernel

Michael Wagman



in collaboration with

Artur Avkhadiev, Phiala Shanahan, and Yong Zhao

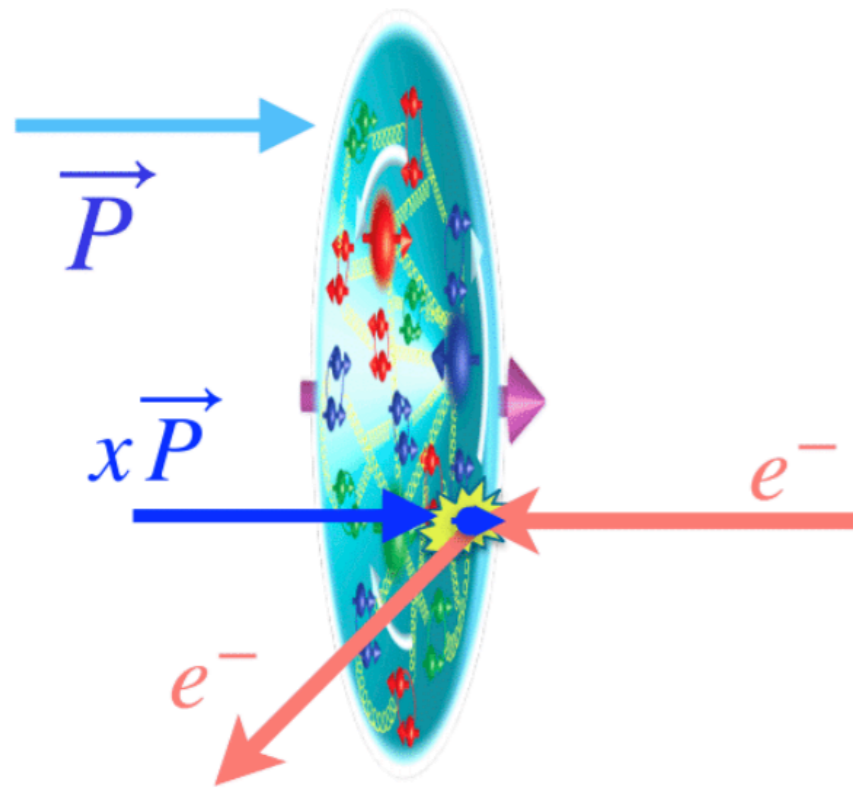
USQCD All Hands Meeting

April 21, 2022



Fermilab

# 3D hadron structure



Our knowledge of proton structure has historically focused on collinear PDFs

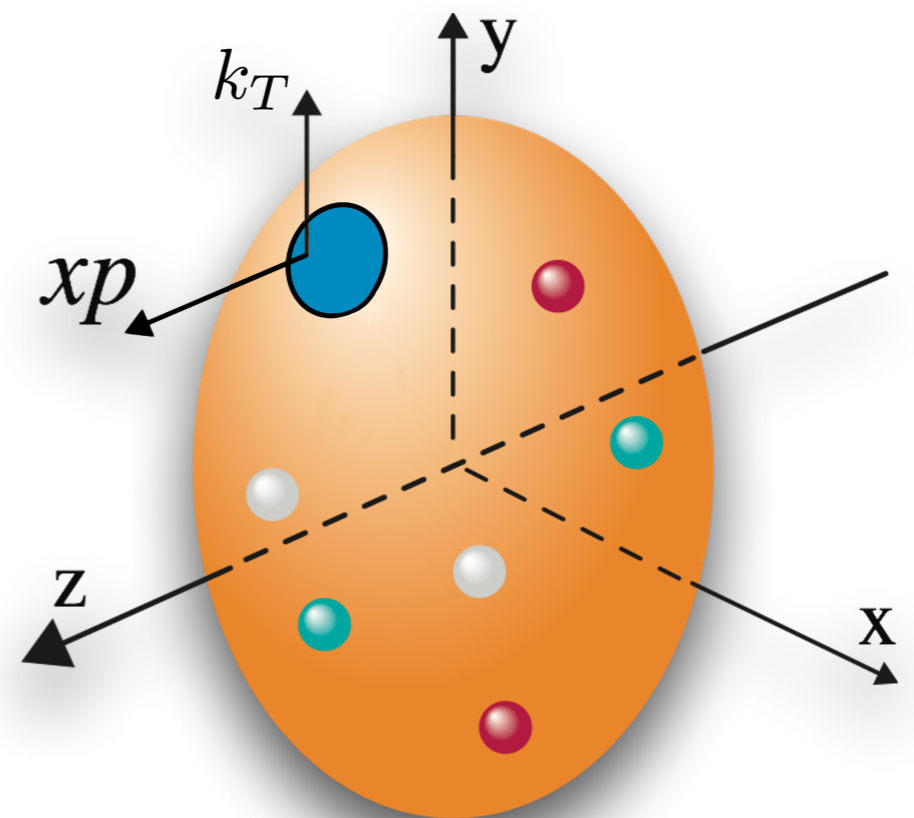
$f_i(x)$  encodes probability of finding a parton of type  $i$  carrying momentum fraction  $x$  within a high-energy hadron

Hadrons further contain rich 3D structure encoded in TMDPDFs

$$f_i(x, \vec{k}_T)$$

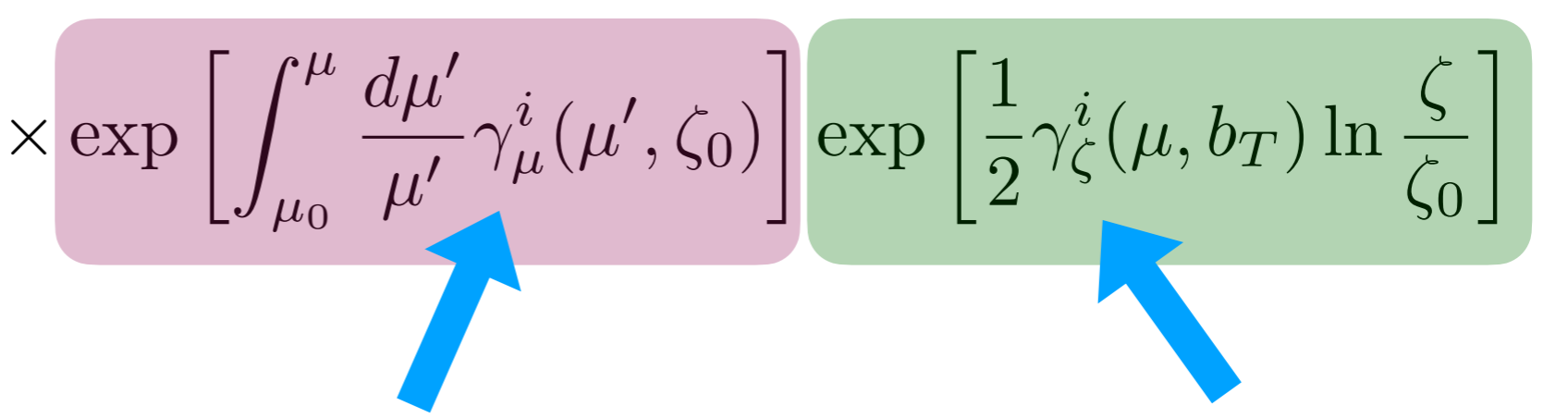
Coordinate-space version:

$$f_i(x, \vec{b}_T) = \int d^2 k_T e^{i\vec{k}_T \cdot \vec{b}_T} f_i(x, \vec{k}_T)$$



# The Collins-Soper kernel

TMDPDFs depend on UV renormalization scale  $\mu$  as well as a scale  $\zeta$  associated with the renormalization of rapidity divergences

$$f_i^{\text{TMD}}(x, \vec{b}_T, \mu, \zeta) = f_i^{\text{TMD}}(x, \vec{b}_T, \mu_0, \zeta_0) \times \exp \left[ \int_{\mu_0}^{\mu} \frac{d\mu'}{\mu'} \gamma_{\mu}^i(\mu', \zeta_0) \right] \exp \left[ \frac{1}{2} \gamma_{\zeta}^i(\mu, b_T) \ln \frac{\zeta}{\zeta_0} \right]$$


UV anomalous dimension                      Collins-Soper kernel  
(rapidity anomalous dimension)

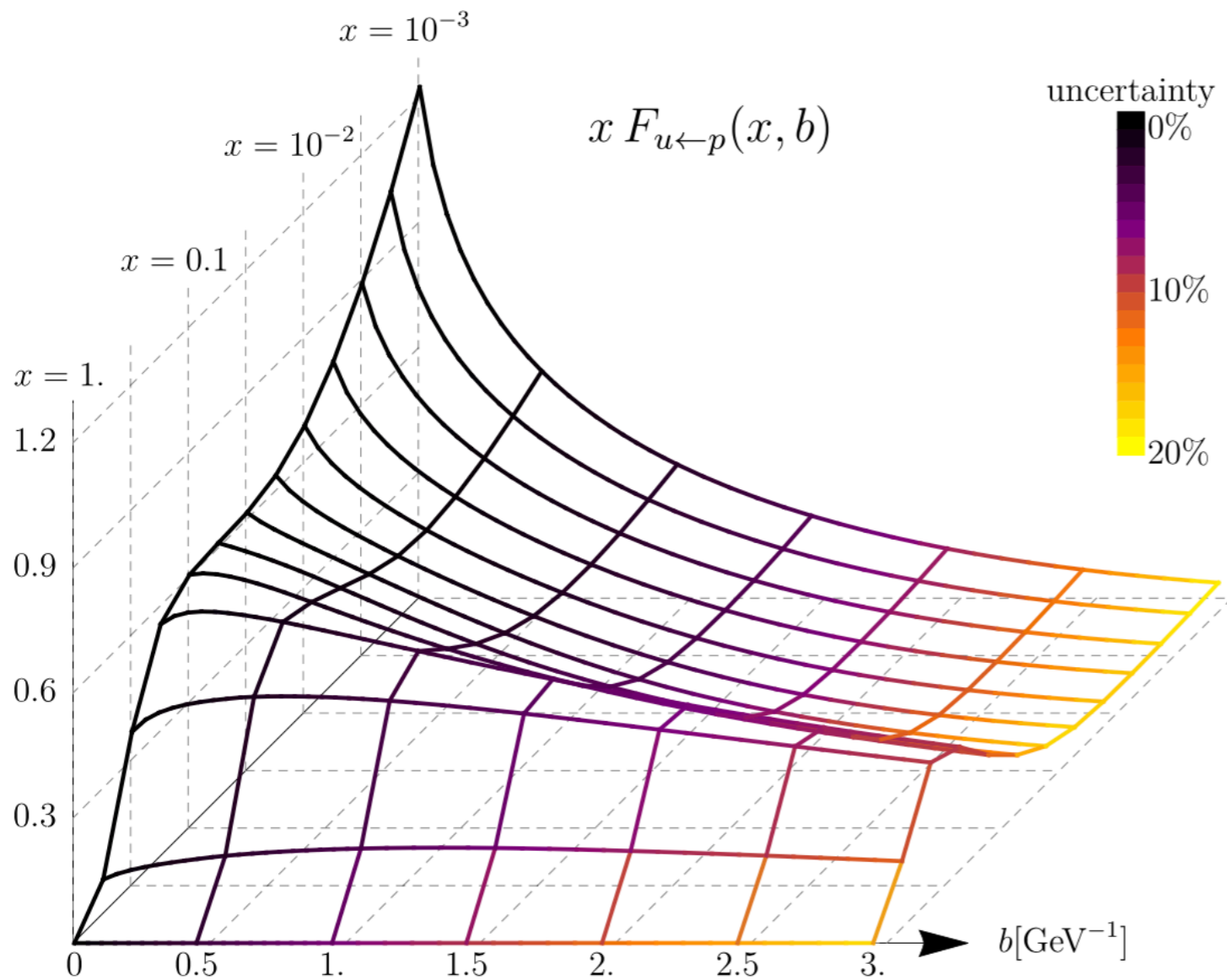
Changing hard momentum scales requires evolving TMDPDFs in  $\mu$  and  $\zeta \sim (2xP^z)^2$

Evolution in  $\mu$  is perturbative as long as  $\mu$  is large, but evolution in  $\zeta$  is always nonperturbative for large  $b_T$

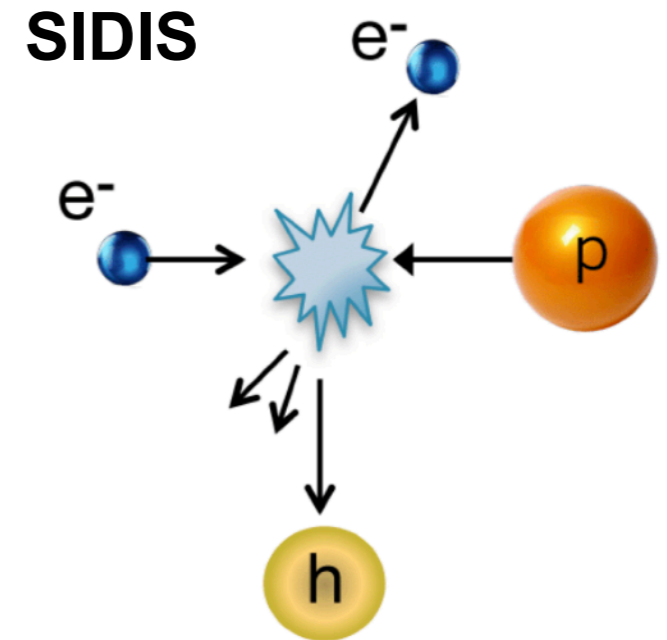
# Experimental probes

TMDPDFs are needed to describe cross-sections for semi-inclusive DIS and the Drell-Yan process

Phenomenological analysis constrain TMDPDFs precisely for small but not large  $b_T$

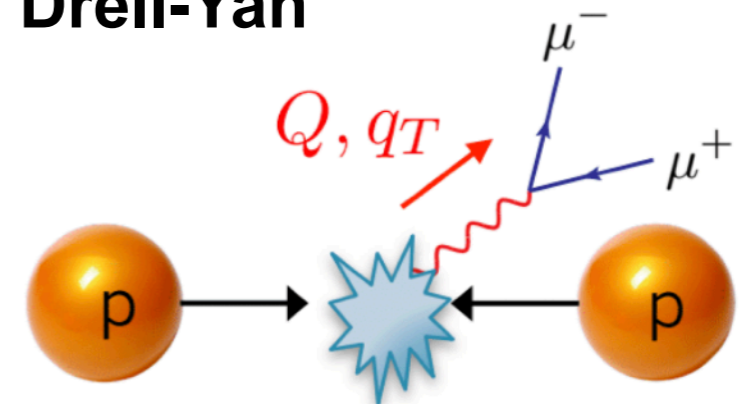


Scimemi and Vladimirov, JHEP 06 (2020)



HERMES, COMPASS, JLab, ...

**Drell-Yan**



Fermilab, RHIC, LHC, ...

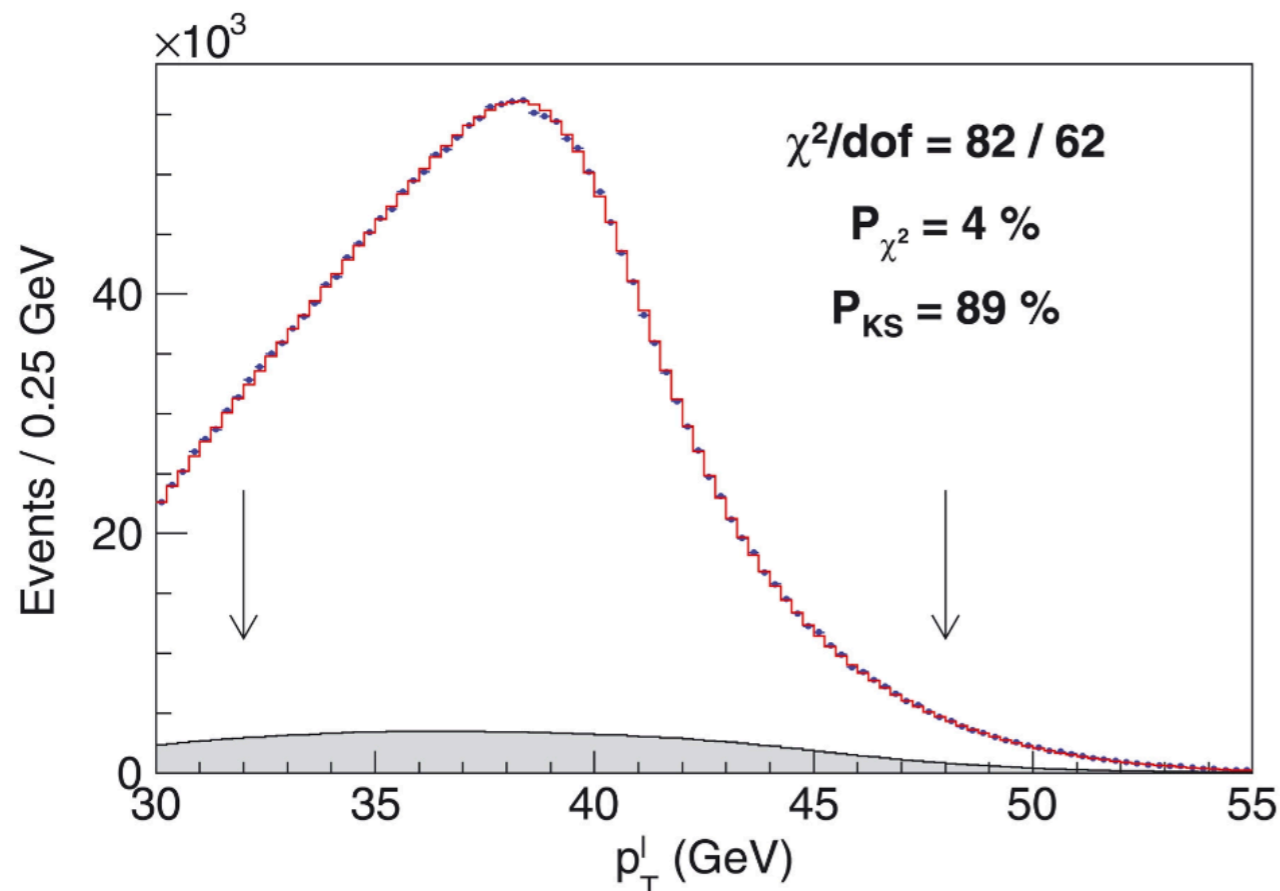
EIC will provide a wealth of data on TMDs in nonperturbative region

# The W boson mass

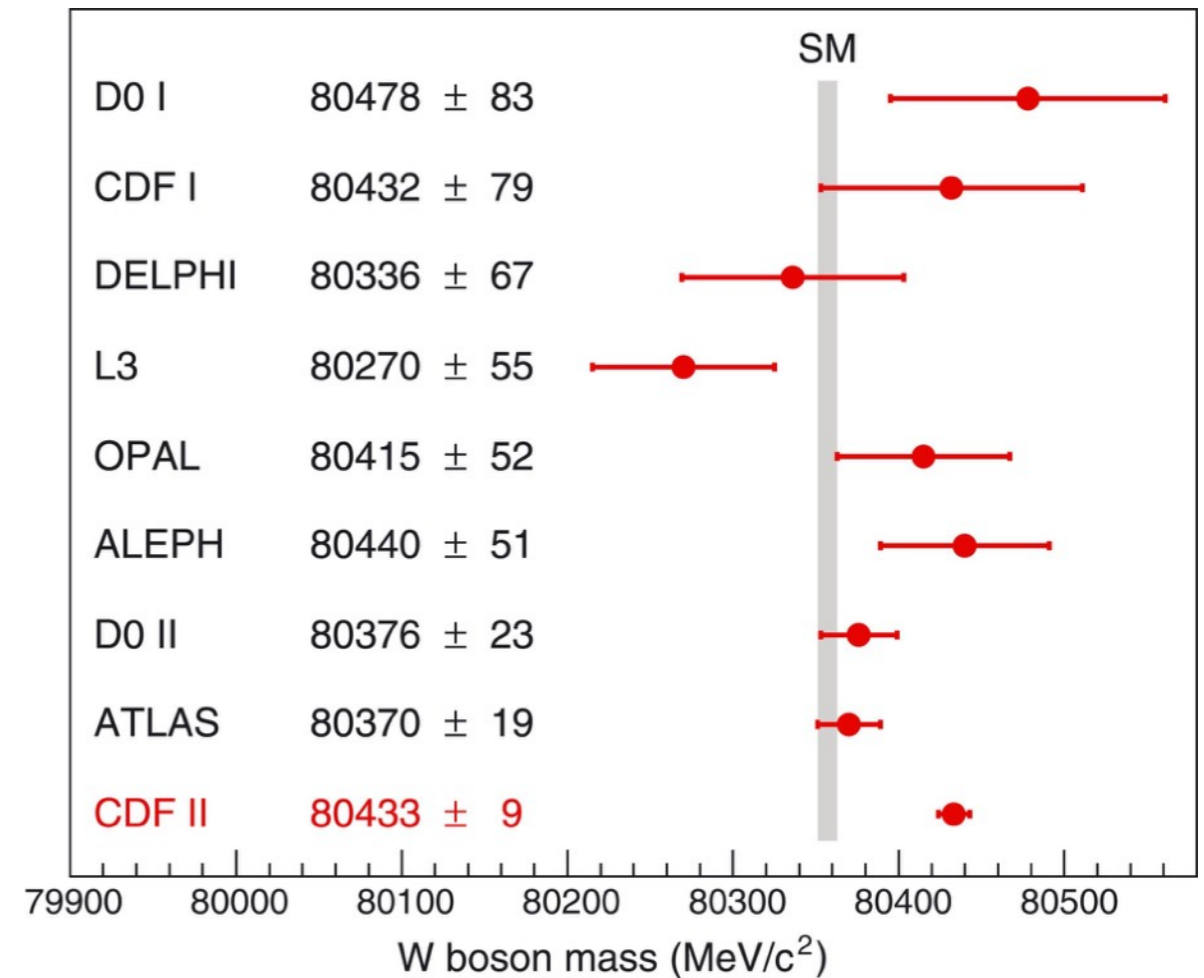
Precise measurement of  $M_W$  from CDF disagrees at 7 sigma with  $M_W$  obtained from electroweak precision fits

New physics?

Robust understanding of all QCD theory uncertainties essential



Aaltonen et al [CDF], Science 376 (2022)



Measurement made by fitting shapes of transverse momentum distributions to theory predictions including resummed and nonperturbative QCD effects

Distribution shapes are insensitive to many aspects of TMDPDFs but are sensitive to flavor dependence and Collins-Soper kernel

# CS kernel phenomenology

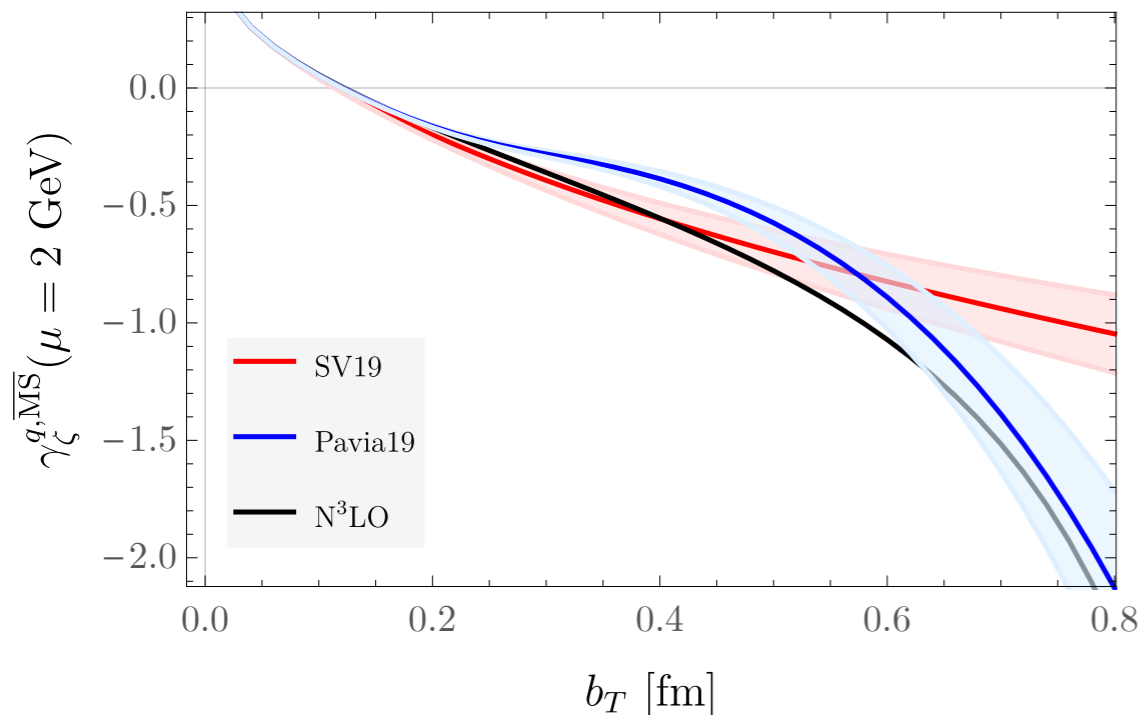
CS kernel can be extracted along with TMDPDF in global fit to DY + SIDIS data

SV19 - Scimemi and Vladimirov, JHEP 06 (2020)

(582 SIDIS + 457 DY data points)

Pavia19 - Bacchetta et al, JHEP 07 (2020)

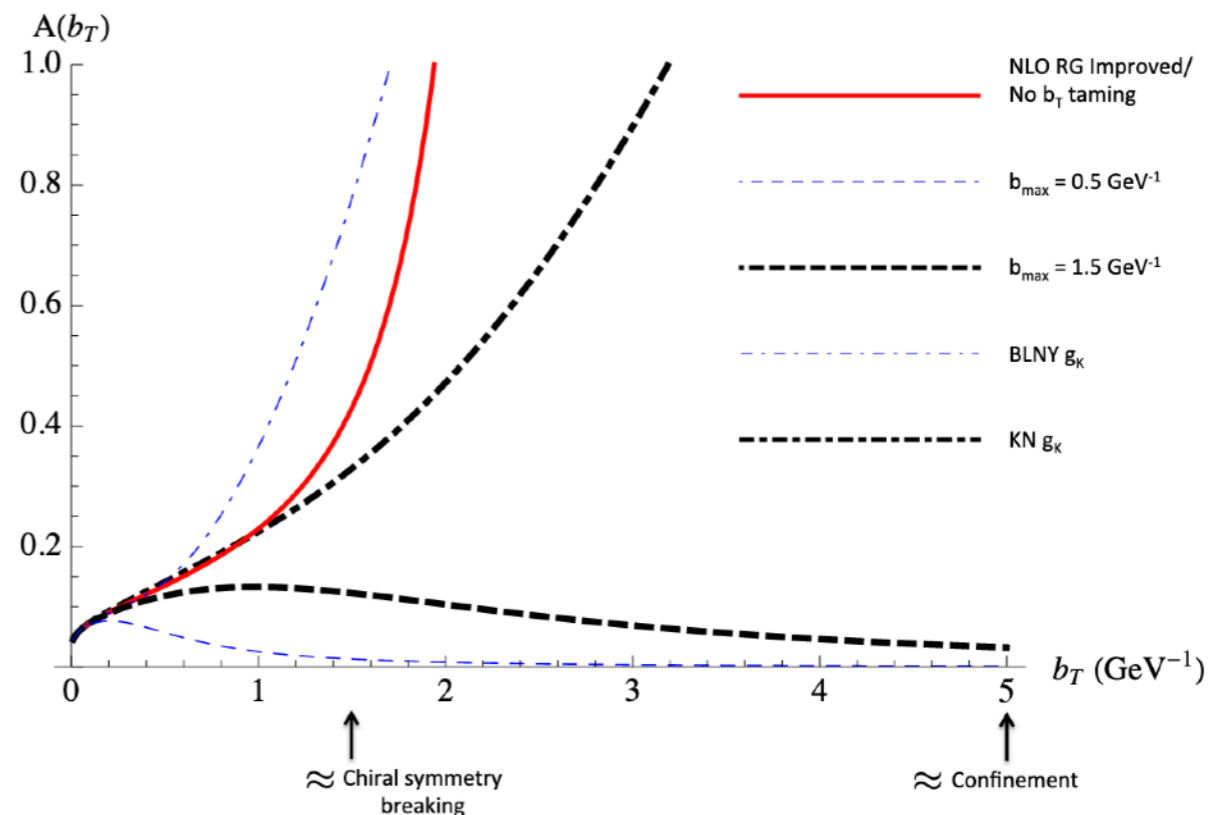
(353 DY data points)



Modeling significant for

$$b_T \gtrsim 0.2 \text{ fm}$$

(nonperturbative region)



Related nonperturbative function

$$A(b_T) = -\frac{b_T}{2} \frac{\partial}{\partial b_T} \gamma_\zeta^q(b_T, \mu)$$

appears in CSS factorization formula used to analyze experimental data (e.g. BLNY used by CDF)

Collins and Rogers, PRD 91 (2015)

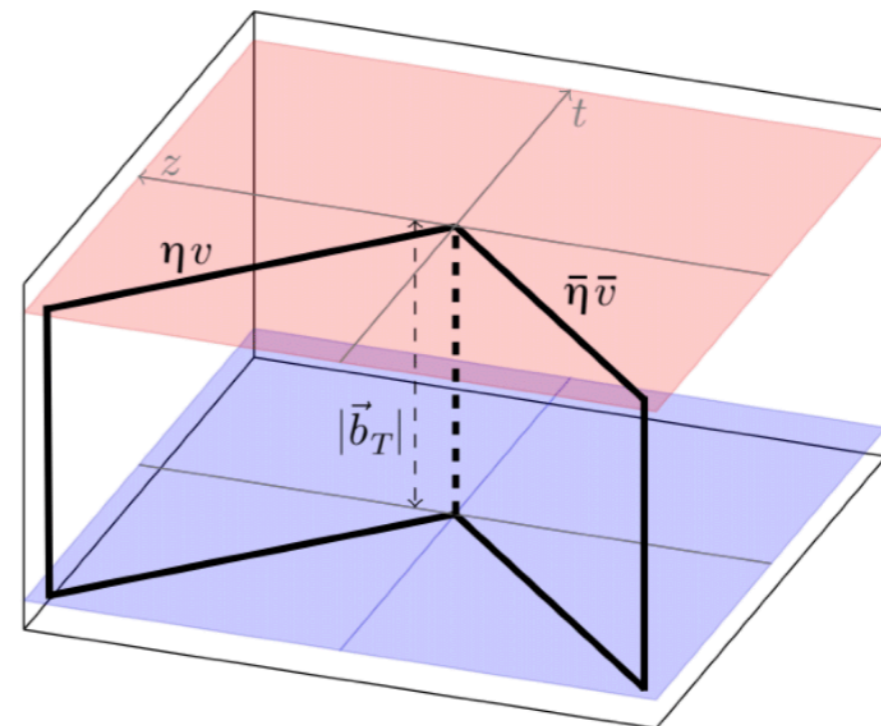
# Quasi TMDPDFs

The construction of quasi TMDPDFs is more complicated than quasi PDFs

Ji, PRL 110 (2013)

TMDPDF products appearing in e.g. Drell-Yan can be expressed as convolutions of “beam functions” and “soft functions”

Soft function cannot be related to a matrix element of equal-time operator product by a Lorentz boost



Ebert, Stewart, Zhao, JHEP 1909 (2019)

Recent progress relating light-cone soft function to a large-momentum form factor that can be calculated with LQCD

Ji, Liu, and Liu, Nucl Phys B 955 (2020)

Zhang et al [LPC], PRL 125 (2020)

# The CS kernel from LQCD

Ratios of TMDPDFs free from soft factors and can be calculated with LQCD

Musch et al, PRD 85 (2012)

Engelhardt et al, PRD 93 (2016)

Yoon et al, PRD 96 (2017)

CS kernel determination using quasi-TMDPDFs suggested

Ji, Sun, Xiong, Yuan PRD 91 (2015)

Method concretely relating CS kernel to quasi TMDPDF ratios proposed and derived

Ebert, Stewart, Zhao, PRD 99 (2019)

$$\begin{aligned} \gamma_{\zeta}^{q, \overline{\text{MS}}} (b_T, \mu) &= 2\zeta \frac{d}{d\zeta} \ln f_q^{\overline{\text{MS}}} (x, b_T, \mu, \zeta) \\ &= \frac{1}{\ln(p_1^z/p_2^z)} \ln \frac{C_{\text{TMD}}^{\overline{\text{MS}}} (\mu, xP_2^z) \int db^z e^{ib^z xp_1^z} \tilde{B}_q^{\overline{\text{MS}}} (b^z, b_T, \eta, \mu, p_1^z)}{C_{\text{TMD}}^{\overline{\text{MS}}} (\mu, xp_1^z) \int db^z e^{ib^z xp_2^z} \tilde{B}_q^{\overline{\text{MS}}} (b^z, b_T, \eta, \mu, p_2^z)} \end{aligned}$$

Euclidean quasi-beam function



# Quenched LQCD exploration

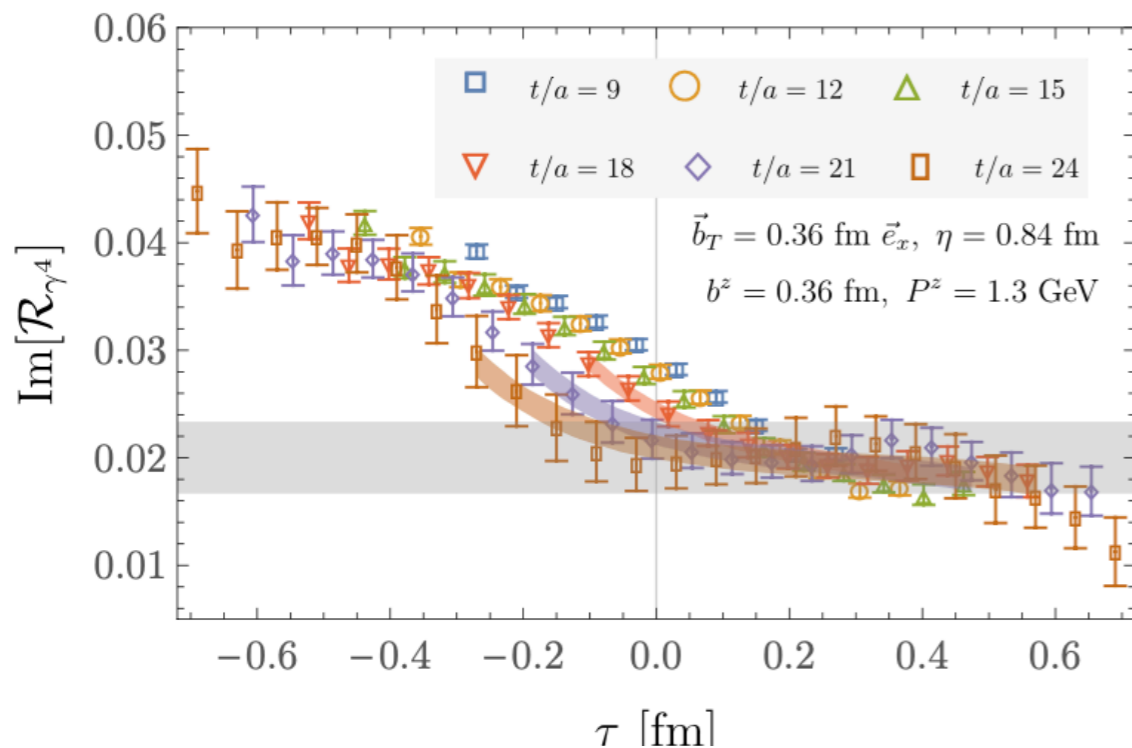
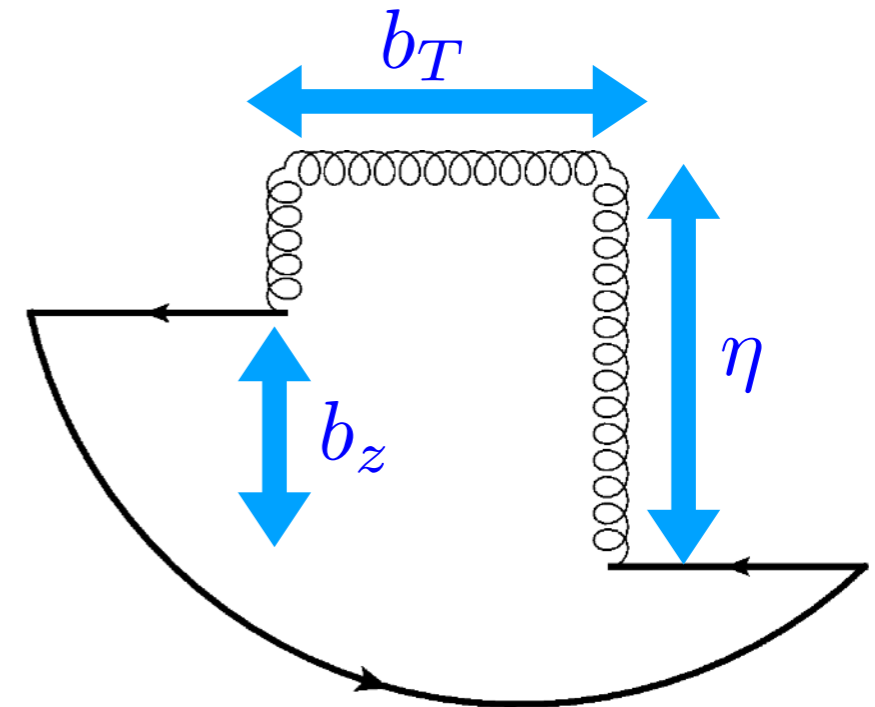
CS kernel property of QCD vacuum,  
independent of hadronic state

## Calculate using pion state

In quenched ( $N_f = 0$ ) QCD, exact results  
calculable using heavy quark probe

$$m_\pi \sim 1.2 \text{ GeV}$$

Allows high precision with only 400 quark propagator sources



Shanahan, MW, Zhao, PRD 102 (2020)

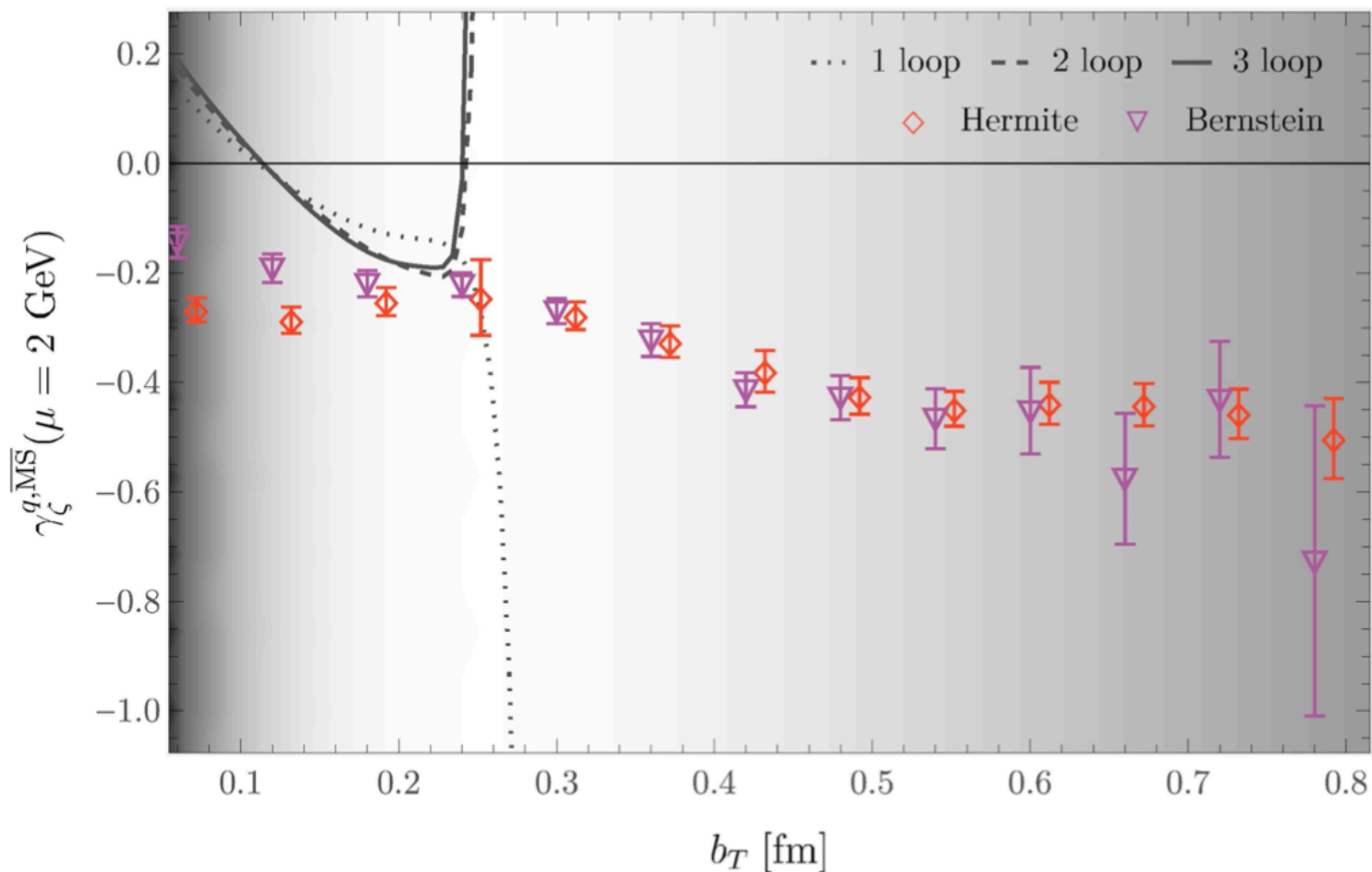
3 values of  $\eta \in [0.6, 0.8]$  fm

3 values of  $P^z \in [1.3, 2.6]$  GeV

All 16 Dirac structures and  
staple geometries  $b_T$  and  $b^z$

35,660 bare matrix elements -  
robust automated fitting essential

# Quenched LQCD results



Shanahan, MW, Zhao, PRD 102 (2020)

Label	$\beta$	$a$ [fm]	$L^3 \times T$	$\kappa$	$n_{\text{src}}$	$n_{\text{cfg}}$
$E_{32}$	6.3017	0.06	$32^3 \times 64$	0.1222	2	200

CS kernel determined precisely for  $b_T$  extending into nonperturbative regime

Fourier transform truncation effects challenging to quantify, two different models used to extrapolate beam functions outside range of data

$$m_\pi = 1.2 \text{ GeV}$$

$$P^z \in \{1.3, 1.9, 2.6\} \text{ GeV}$$

$$\eta \leq 0.8 \text{ fm}$$

# $N_f = 2 + 1 + 1$ LQCD calculation

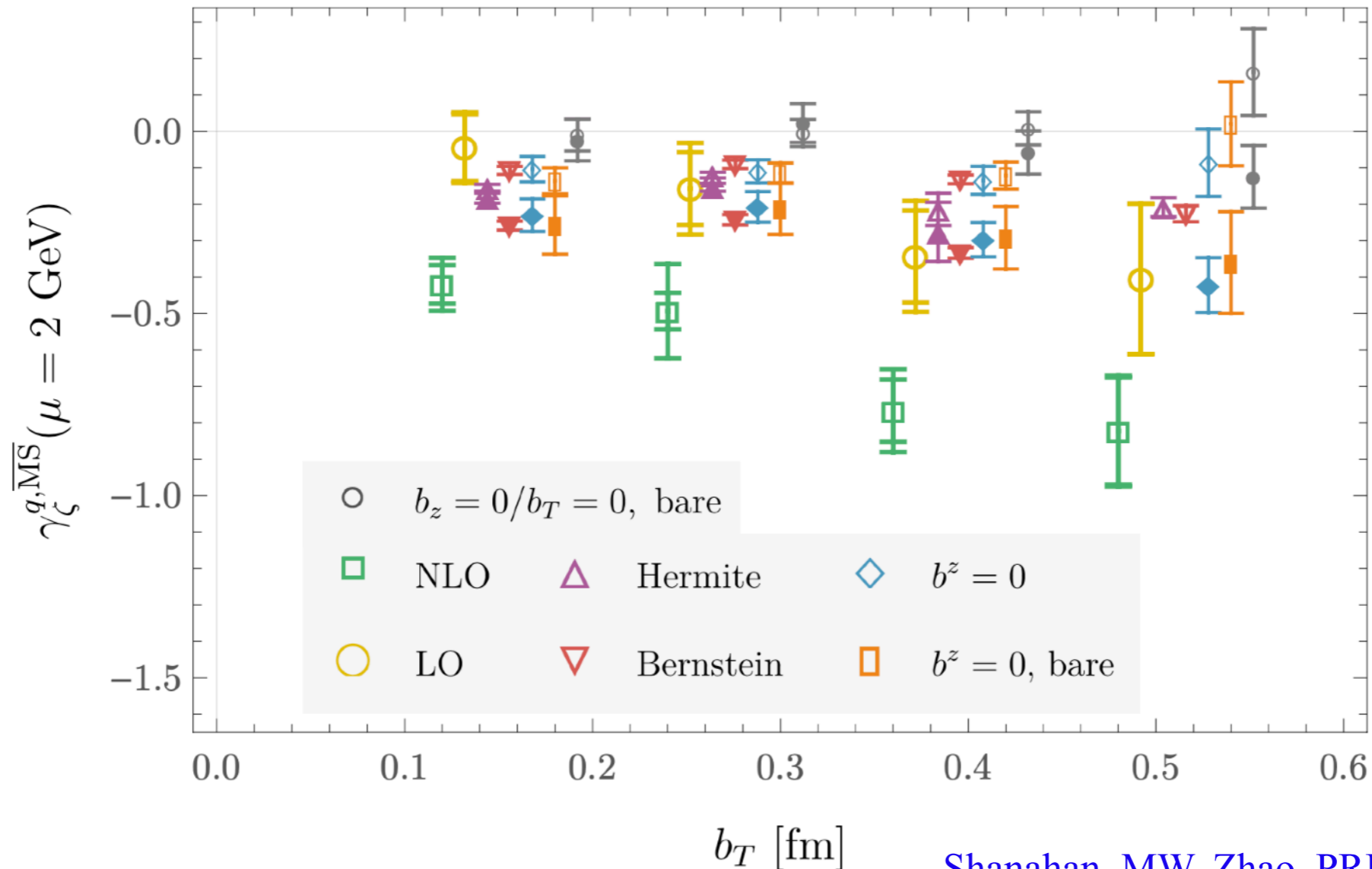
Shanahan, MW, Zhao, PRD 104 (2021)

HISQ lattices from MILC, gradient flowed,  
with clover valence quarks

- ✓ NLO matching from quasi- to light-cone beam functions
- ✓ Demonstration of  $x$  independence of CS kernel
- ✓  $\overline{\text{MS}}$  renormalization + operator mixing using RI/MOM  
(quark vs pion static quark potential correction applied)
- ✓ Fourier transformation to  $x$  - space
- ✓ Finite-momentum power corrections studied
- ✓ Unphysically heavy valence quark mass

# Comparing approximations

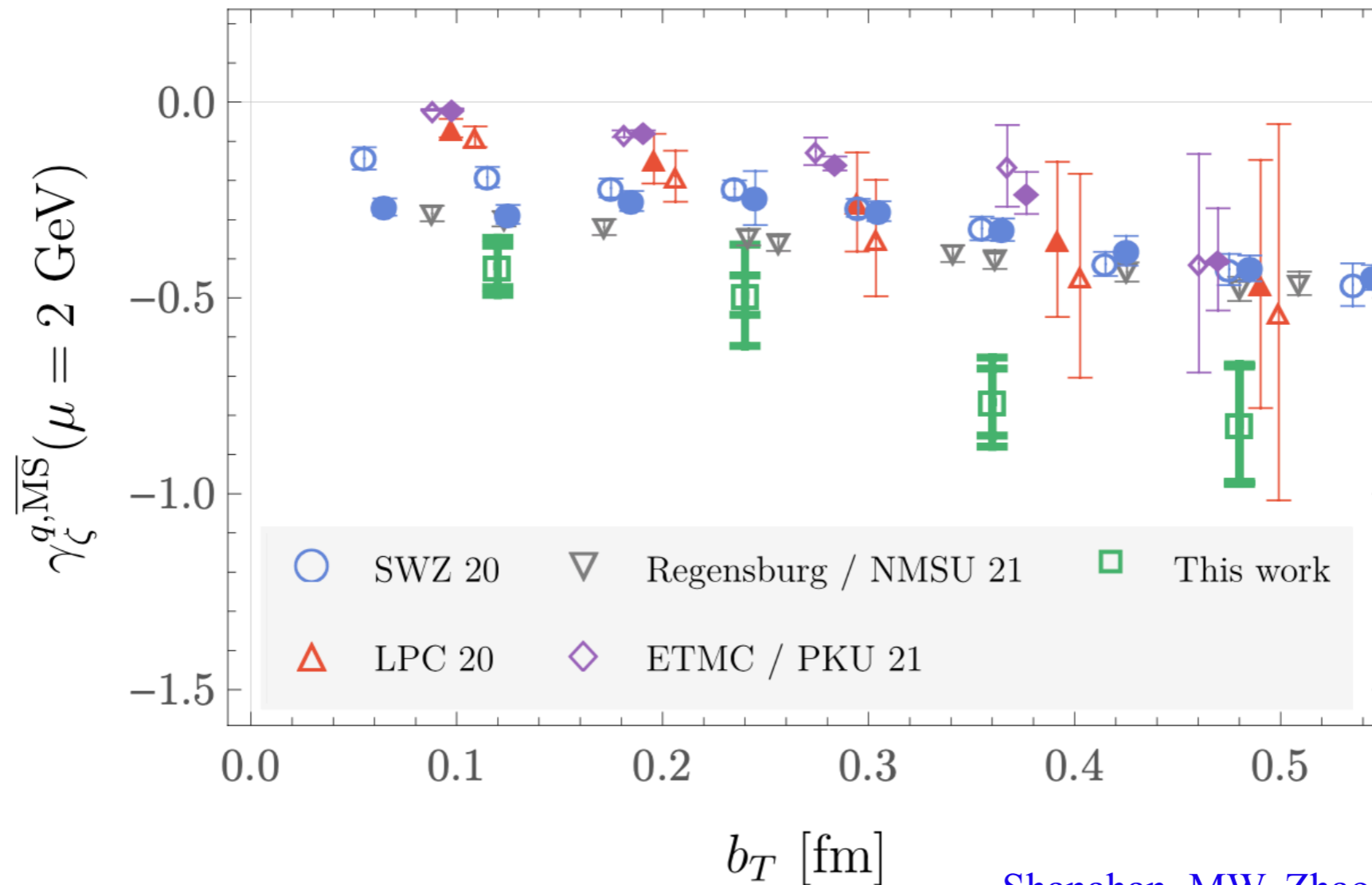
NLO matching leads to significant effects on CS kernel determination



LO results using ratios of  $b^z = 0$  beam functions or the momentum-space models used in quenched calculation are consistent with LO results using average over  $x$  dependence but give smaller uncertainty estimates

# Lattice comparison

Results are broadly consistent with other LQCD calculations (different actions and systematics)



Shanahan, MW, Zhao, PRD 104 (2021)

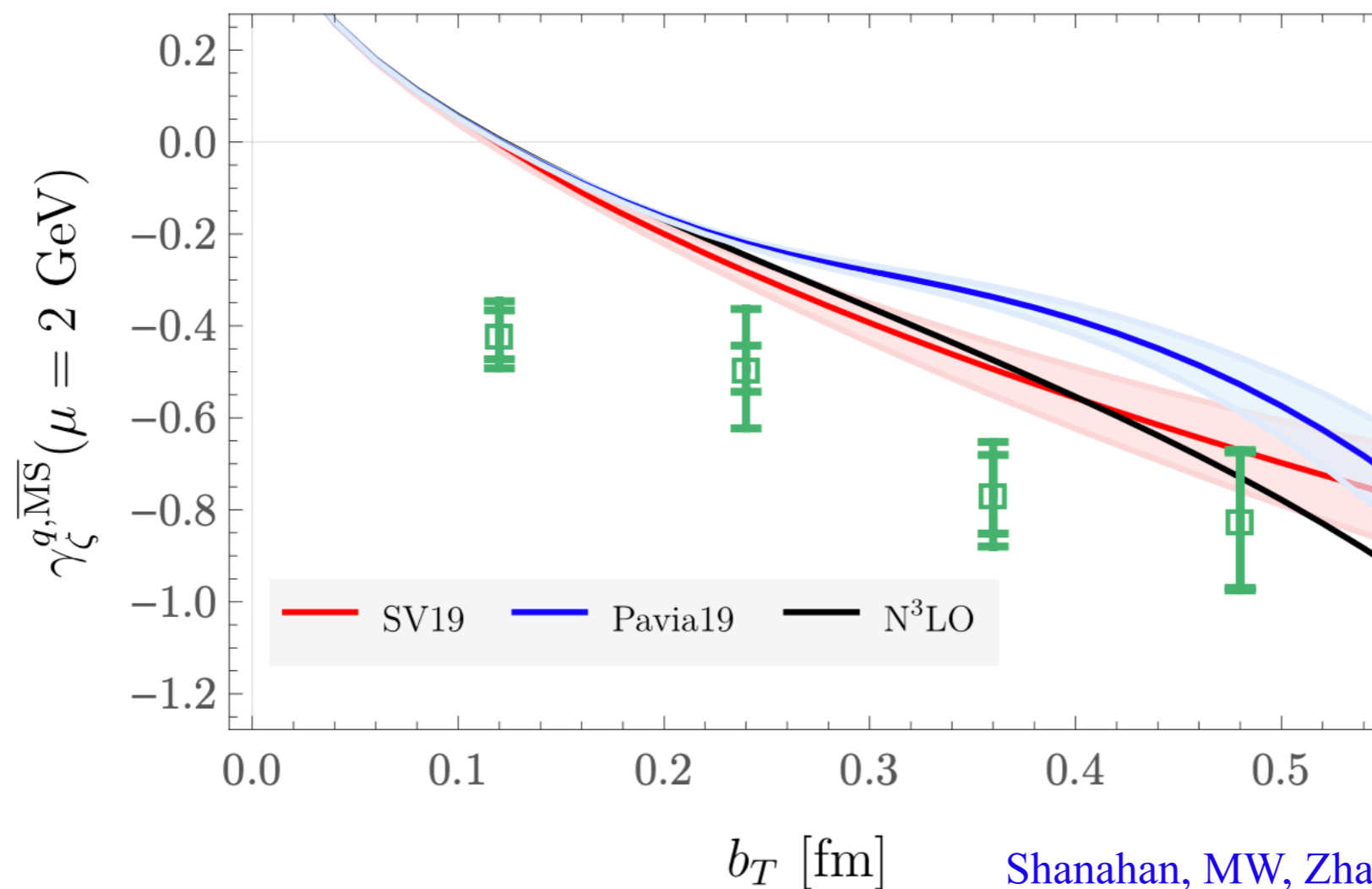
Differences with previous LO calculations (SWZ 20, LPC 20, ETMC / PKU 21) consistent with differences between Fourier transform schemes

See also Chu et al [LPC] arXiv:2204.00200

# Phenomenological comparison

Current LQCD results can also be compared with phenomenology

**Warning - no continuum extrapolation, unquantified systematics remain**



Lattice artifacts at small  $b_T$ ? Underestimated Fourier transform systematics?  
Further studies needed!

# Large-distance extrapolation

Fourier transforming data from a finite interval is a formally ill-posed problem

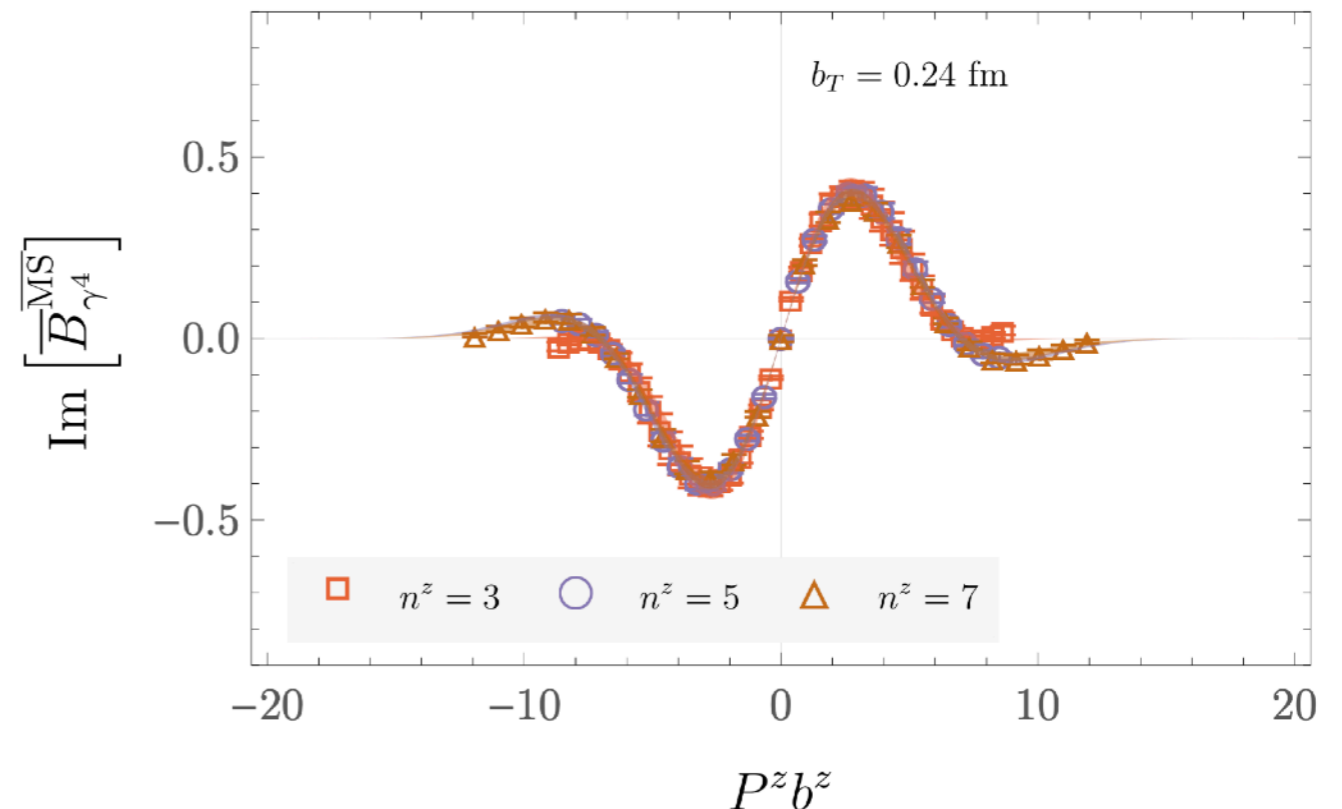
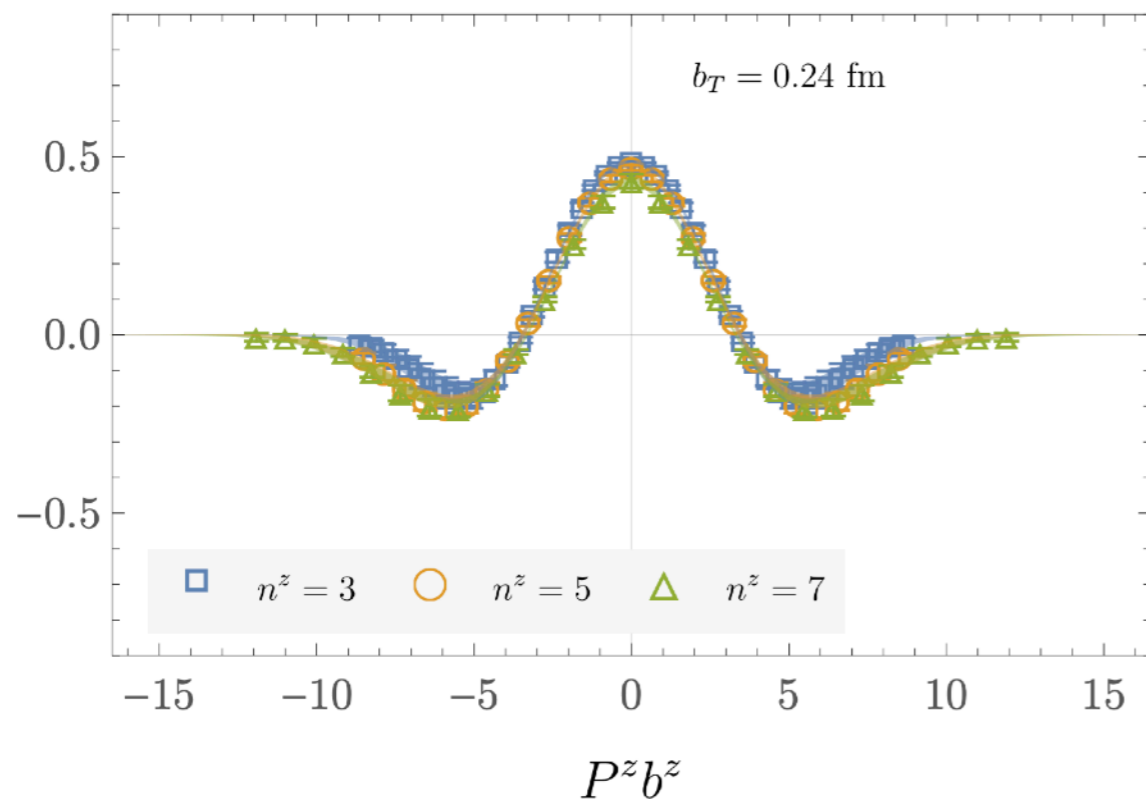
LQCD results span a finite range of

$b^z, P^z,$

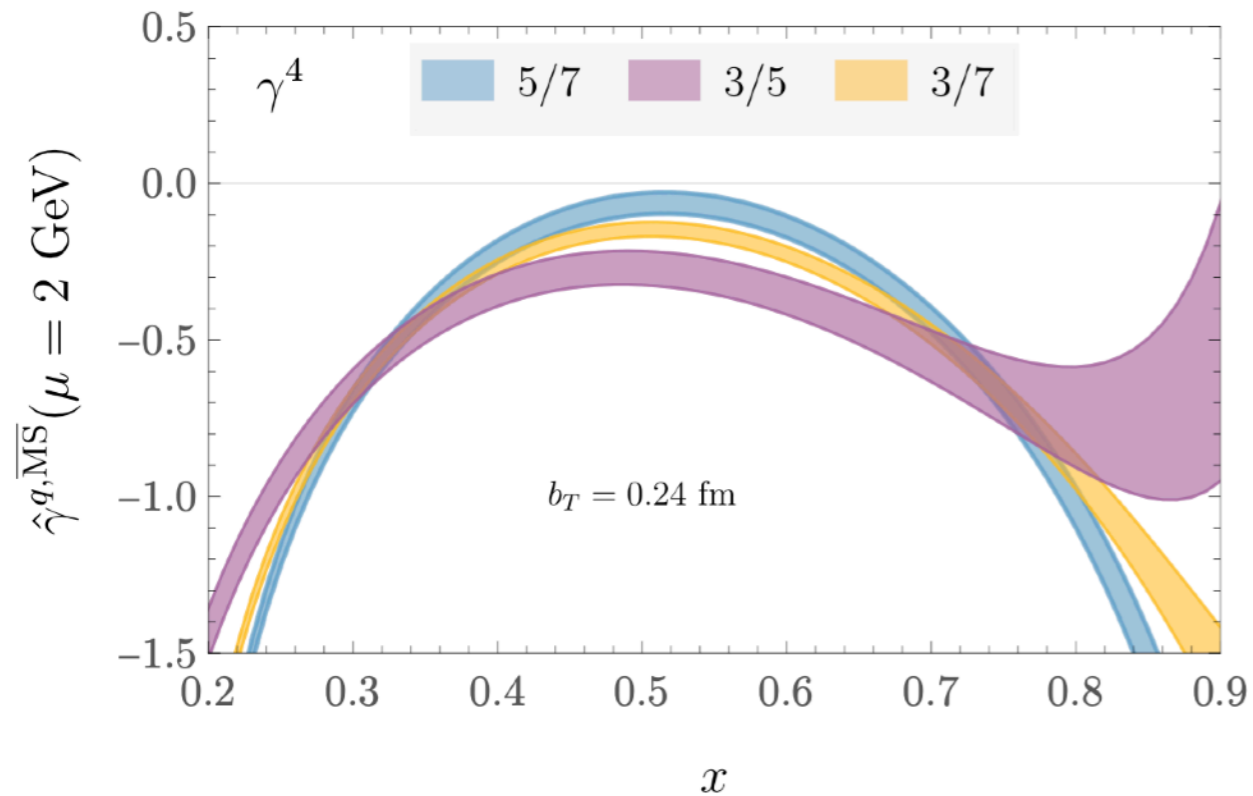
$$b \cdot P = b^z P^z$$

Fourier conjugate to  $\mathcal{X}$

Fits performed independently for each  $b_T, P^z$  to analytic model in order to extrapolate to larger  $b^z$



# CS kernel systematics



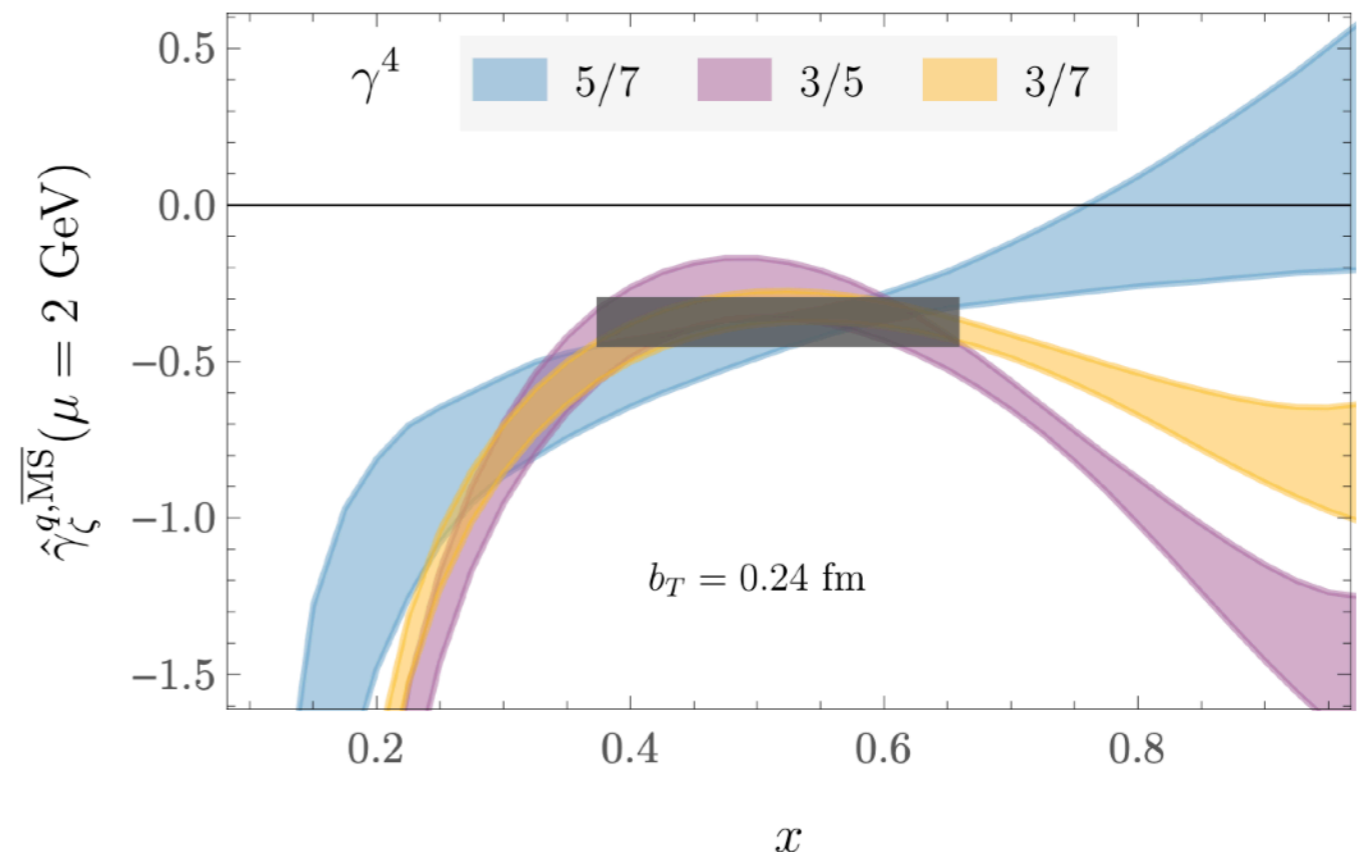
Discrete Fourier transform leads to significant  $x$  dependence of (asymptotically flat) CS kernel estimate

Differences between estimates with different momentum pairs visible

Fourier transforming the analytically extrapolated model leads to smaller (though still visible)  $x$  and  $P^z$  dependence

“Plateau region” identified by automated search for overlap between different  $P^z$  pairs

Fits of  $1/P^z$  artifacts also attempted





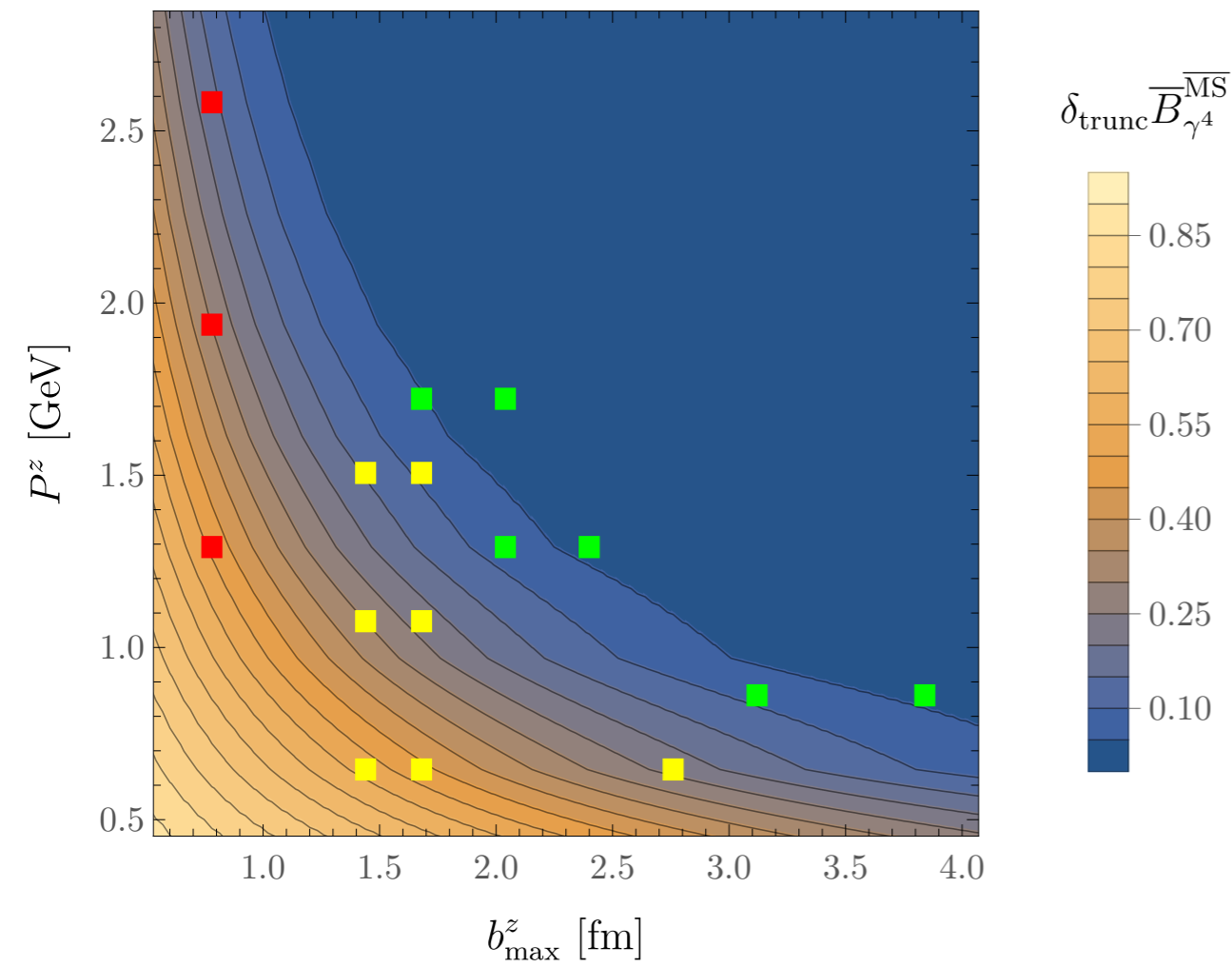
# Proposed calculations

TMDPDF evolution effects can be determined from ratios of TMDWFs analogous to distribution amplitudes

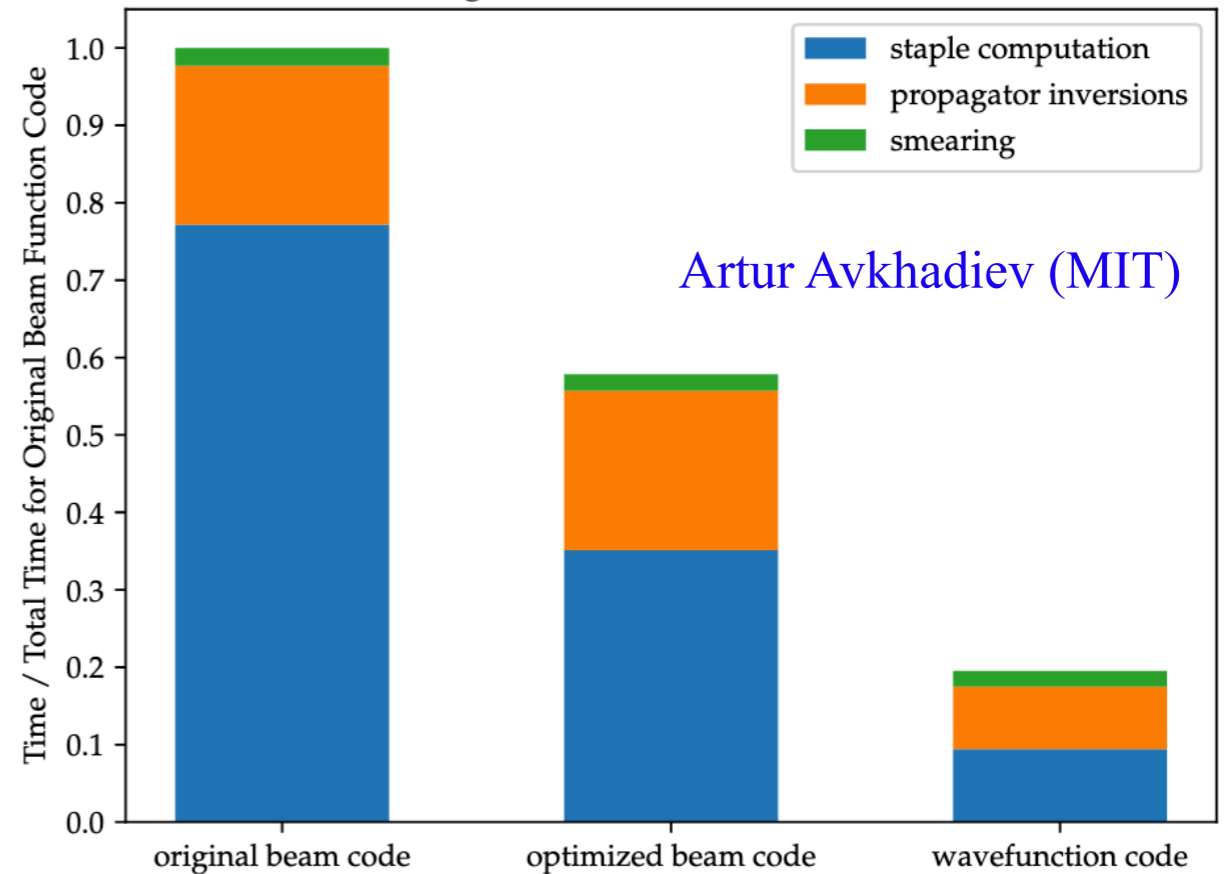
$$\tilde{\psi}(b^z, b_T, \eta, P^z) \propto \langle 0 | \mathcal{O}(b^z, b_T, \eta) | \pi(P^z) \rangle$$

Preliminary studies suggest TMDWFs will enable significantly more efficient CS kernel calculations

$$b_T = 0.36 \text{ fm}$$



Timings for Beam and Wavefunctions



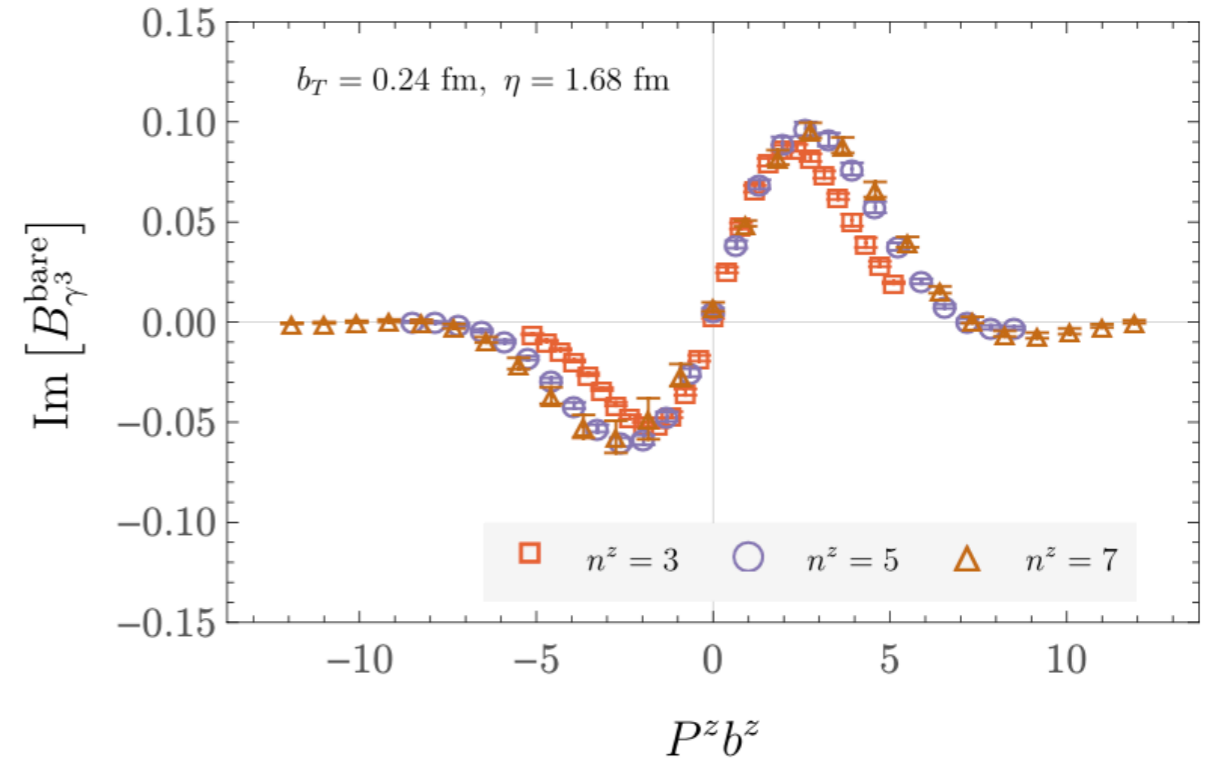
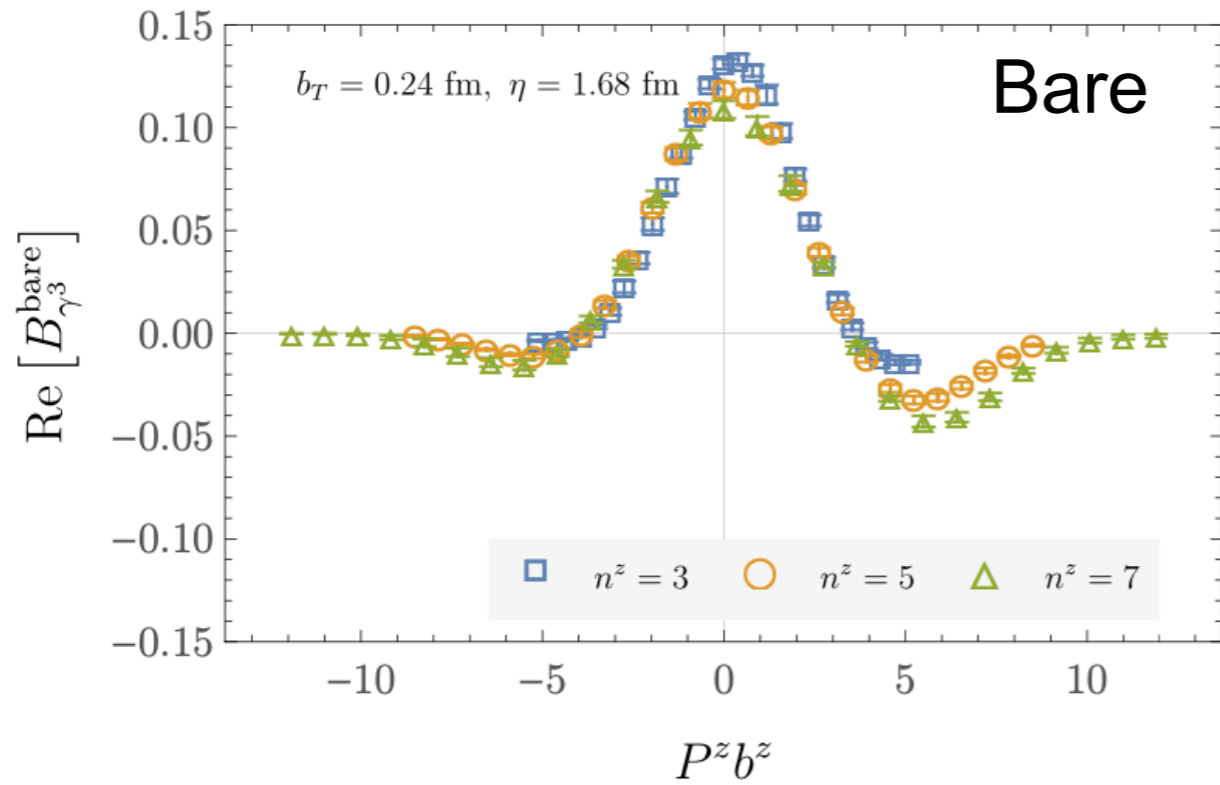
Artur Avkhadiev (MIT)

New formal and code developments provide several improvements:

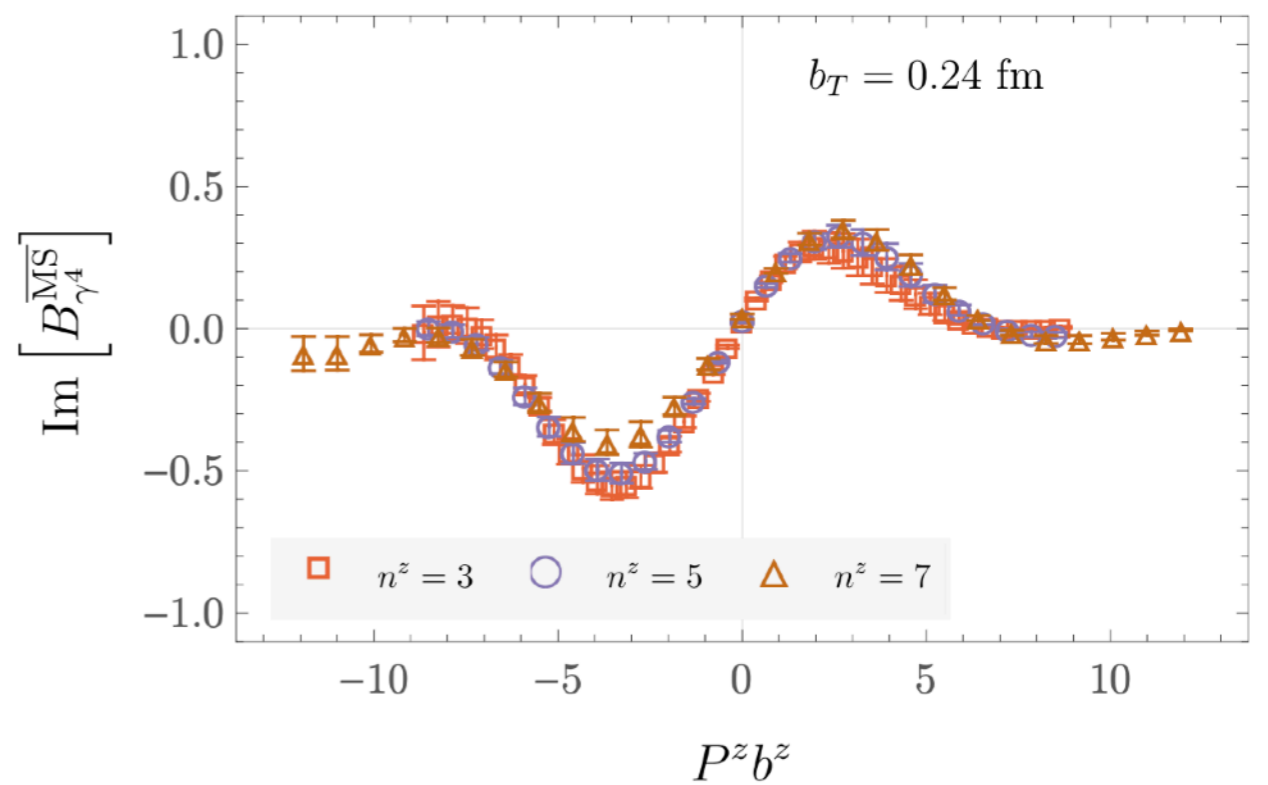
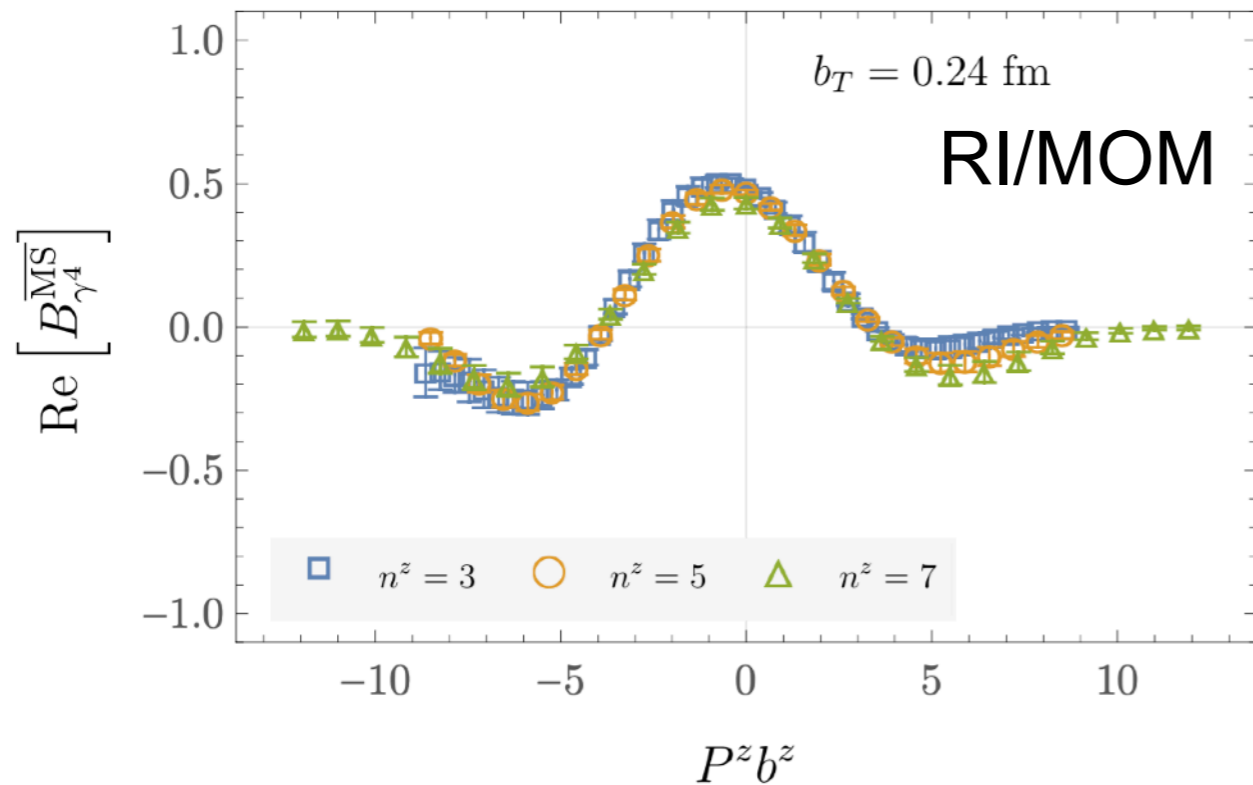
- Larger  $b^z P^z$  with similar truncation effects for all  $P^z$
- Robust nonlocal operator renormalization
- Approximately physical quark masses

# Backup

# Trouble with RI/MOM



Asymmetry visible in beam functions after RI/MOM renormalization



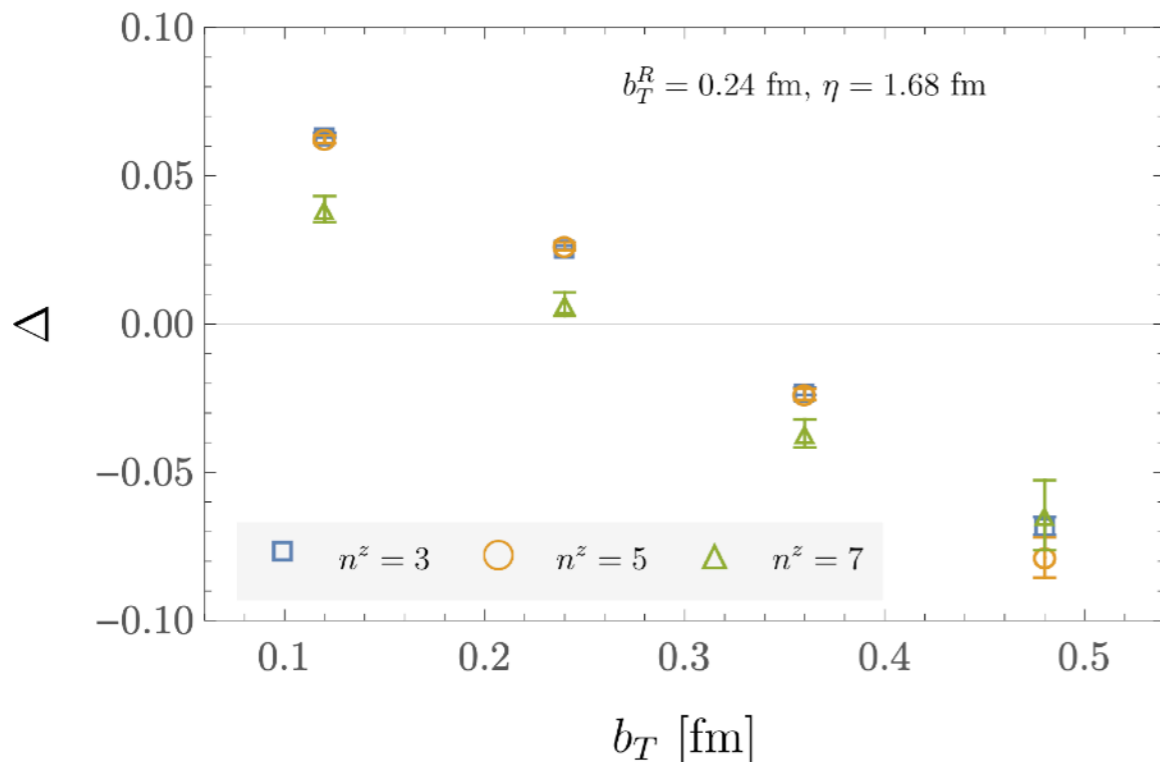
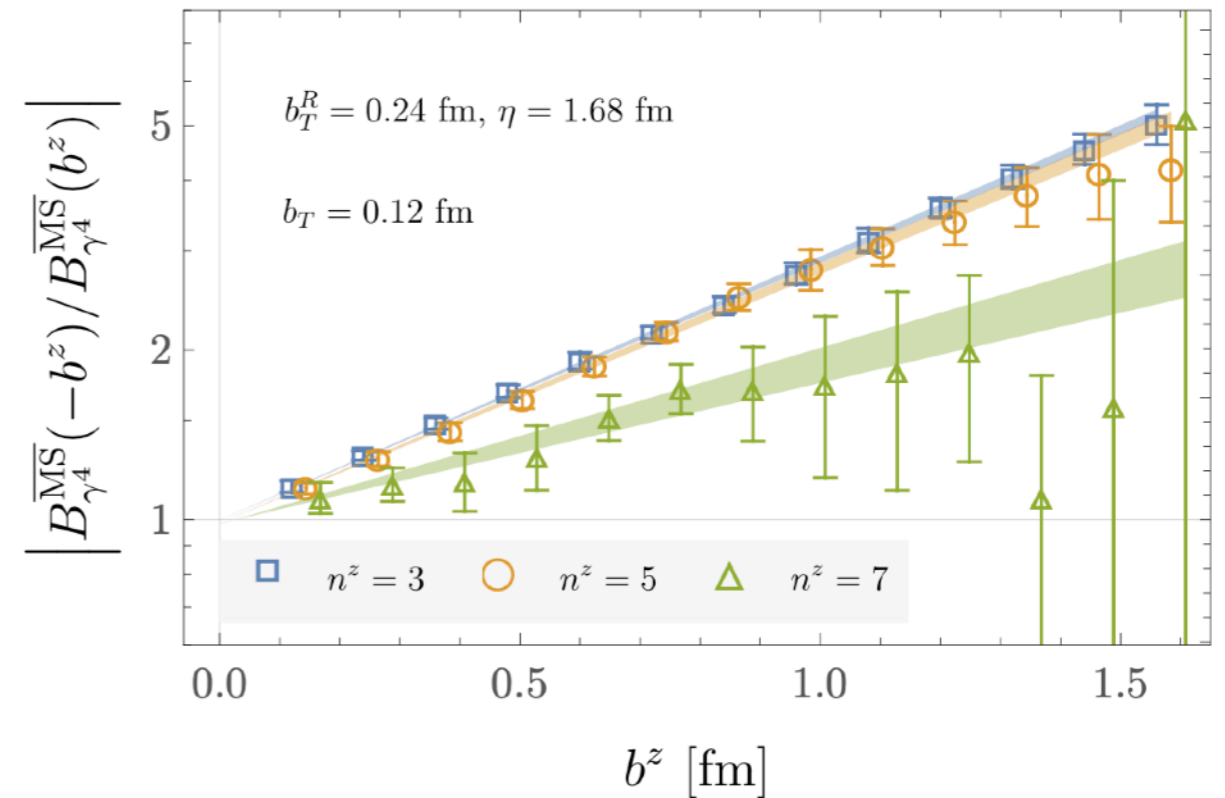
# Beam function asymmetry

Asymmetry visible after RI/MOM renormalization could arise from state-dependence of static quark potential

State dependence of static quark potential also visible in previous calculations

Zhang et al [χQCD], PRD 104 (2021)

Huo et al [LPC], Nucl. Phys. B 969 (2021)



Correction for difference in static quark potentials applied

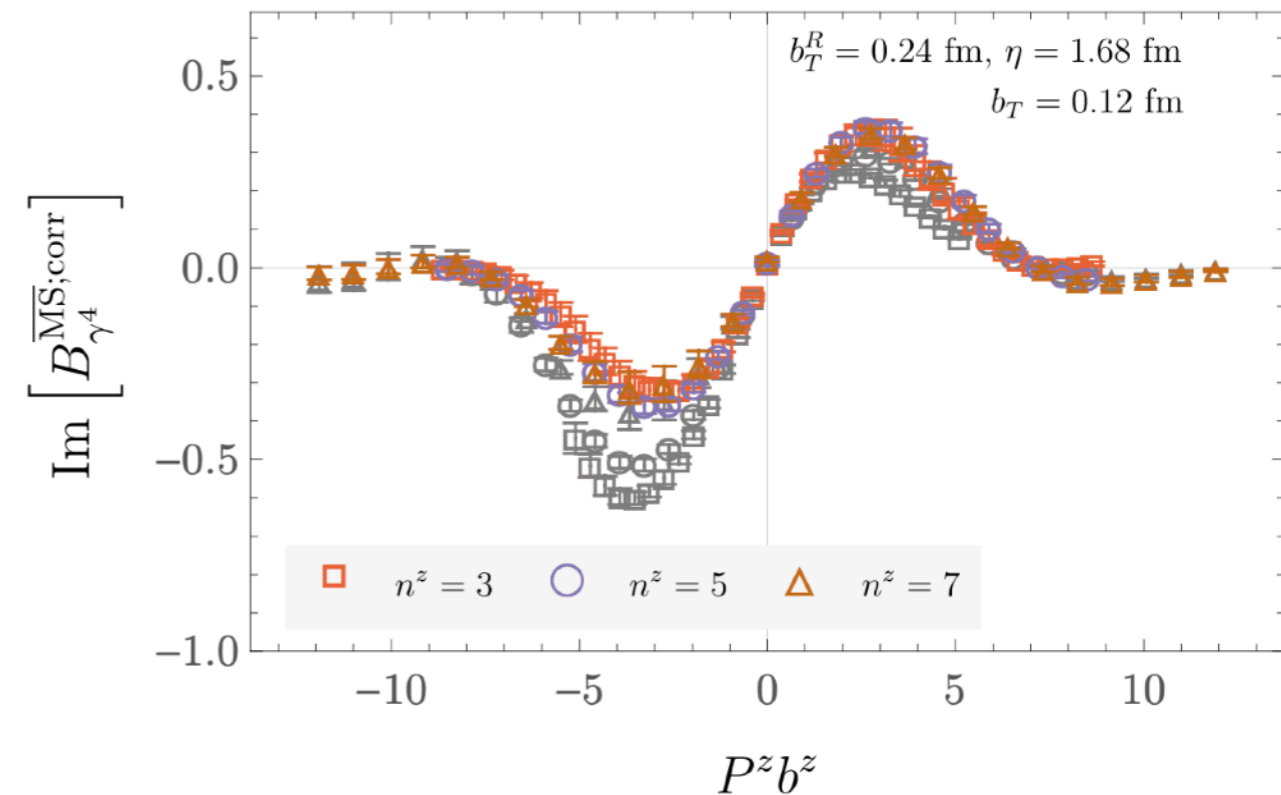
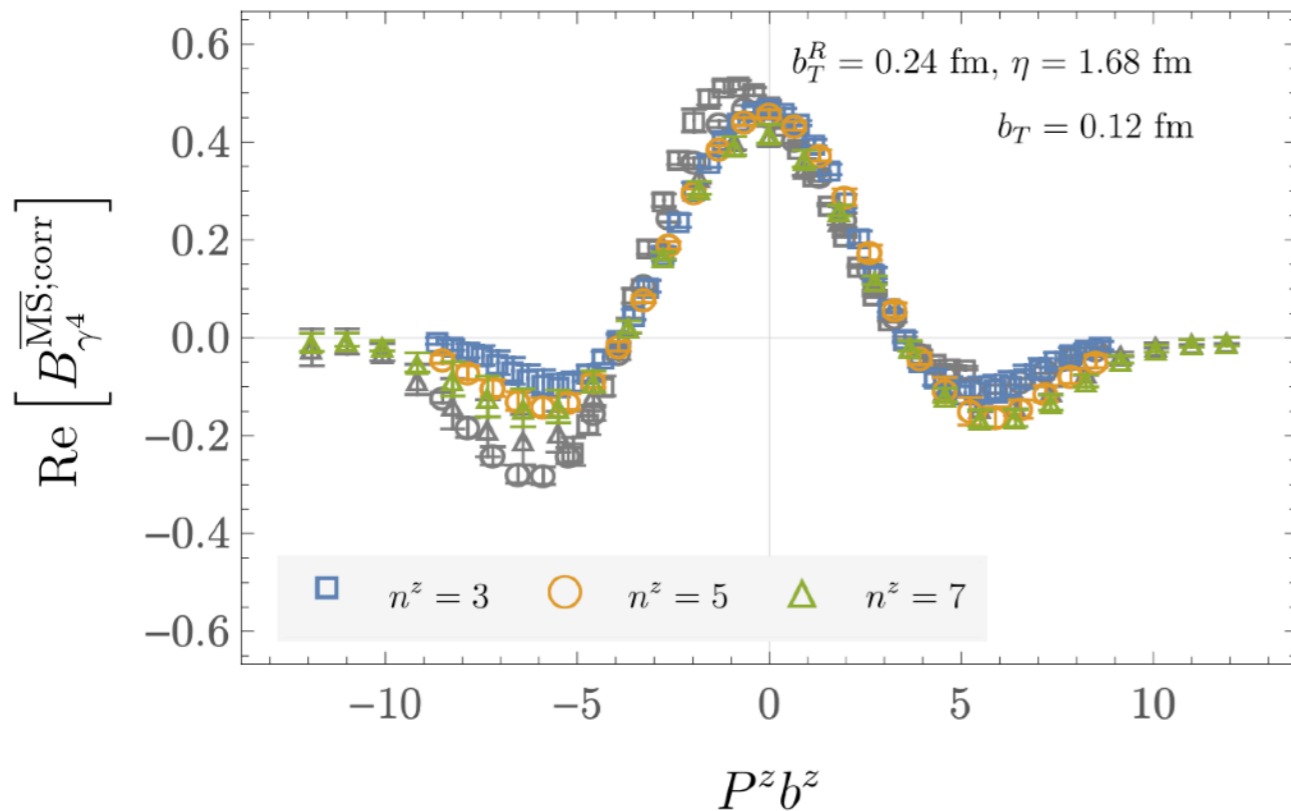
$$B_{\gamma_4}^{\overline{MS};\text{corr}}(b^z, b_T) = e^{\Delta(b_T)|b^z|} B_{\gamma_4}^{\overline{MS}}(b^z, b_T)$$

Roughly linear trend in  $b_T$  observed

$$\Delta(b_T) = V(b_T)_{\text{quark}} - V(b_T)_{\text{pion}} \sim \sigma b_T$$

# Asymmetry correction

After correcting for state dependence of static quark potential, expected (anti)symmetrization of beam function emerges



Extrapolation to large  $\eta$  (by a constant) and averaging over choice of  $b_T^R$  used in renormalization performed after including corrections independently

Systematics included to reflect variation in  $\eta$  and  $b_T^R$  reduced after corrections included